Supplemental Table S1. Primer sequences used for genetic and qPCR analyses.

Target	Purpose	Primer ID	Primer Sequence
XXT1	T-DNA Screening	*XXT1* LP	GAAATCTCGAGACCGGACTAATAAACCT
		XXT1 RP	ATCCCCCAATAACCGTGCAAGTAATAAC
XXT2	T-DNA Screening	*XXT2* LP	CCAAAGAGCTTTACGCCAAT
		XXT2 RP	CGCTTGTTAGGTCCGATGAA
XXT5	T-DNA Screening	*XXT5* LP	GATGAGCCTCAGGAAGGTGA
		XXT5 RP	CATCACGAATTGGCCCTTTA
SAIL T-DNA	T-DNA Insert	LB3	TAGCATCTGAATTTCATAACCAATCTCGATACAC
SALK T-DNA	T-DNA Insert	LBb1.3	ATTTTGCCGATTTCGGAAC
GABI-kat T-DNA	T-DNA Insert	GABI LB 8760	GGGCTACACTGAATTGGTAGCTC
XXT1	qPCR	*XXT1* qLP	GGAGACAATCAGATCCTTCAAATGT
		XXT1 qRP	ATTGCGCGTGGGTTTCAC
XXT2	qPCR	*XXT2* qLP	CATTTCCACGCACGCAAAC
		XXT2 qRP	CCGTCACCGGAAGAAGAATC
XXT5	qPCR	XXT5 qLP	GATGCTTGGGCGCCTATG
		XXT5 qRP	CAATACCTTCCCGGCCTCAT
PDF2	qPCR	*PDF2* qLP	TAACGTGGCCAAAATGATGC
		PDF2 qRP	GTTCTCCACAACCGCTTGGT

Supplemental Data: Col-0 and Mutant Transcript Characterization

Supplemental Results and Discussion

Analysis of the *xxt1 xxt2 xxt5* triple mutant cDNA by RT-PCR showed that there was an absence of *XXT1*, *XXT2*, and *XXT5* transcripts when gene-specific primers (GSP) flanking the T-DNA insert were used (Fig. 1D). Although these mutants did not produce wild-type (WT) transcripts, it is possible that they could have produced functional chimeric transcripts (Wang, 2008 and references therein). Therefore, to determine if chimeric transcripts were present we employed RT-PCR with gene-specific primers and the respective left border (LB) or right border (RB) T-DNA border primer combinations (Supplemental Table S1). Results from these experiments showed the presence of chimeric transcripts for all three mutant genes in the *xxt1xxt2xxt5* mutant (Supplemental Fig. S1). The *xxt1* and *xxt5* genes produced chimeric transcripts that have LB border sequences on the 5' and 3' sides of the T-DNA insert (Fig. 1A and 1C). Although, the *xxt2* chimeric transcript has a LB on the 3' side of the T-DNA insert, we could not identify the 5' T-DNA using combinations of gene-specific primers and either of the alternative LB primers suggested. (http://signal.salk.edu/tdnaprimers.2.html) or custom designed RB primers (Supplemental Table S1 and Supplemental Fig. S1). PCR amplicons from the chimeric transcripts were sequenced and aligned with the respective gene (Fig. 1C) to determine the precise location of the T-DNA border and the number of stop codons present in all reading frames. With the exception of the 5' side of the *xxt2* T-DNA insertion, the T-DNA insertion introduced multiple stop codons in all three reading frames.

We employed qPCR using primer combinations (Supplemental Table S1) located on the 3' end of each gene to measure transcript levels in the WT (*XXT1*, *XXT2*, and *XXT5* in Col-0) and mutant (*xxt1*, *xxt2*, and *xxt5* in the triple mutant) in the same cDNA samples used for the RT-PCR and sequencing experiments presented above. There were no statistical difference in expression of *XXT1* in Col-0 and the *xxt1* chimera in the *xxt1 xxt2 xxt5* triple mutant. However, there are significant reductions ($P < 0.01$) in the expression of the *xxt2* and *xxt5* chimeras in the *xxt1 xxt2 xxt5* mutant when compared to Col-0 (Supplemental Fig. S2). Thus, the *xxt1xxt2xxt5* mutant is producing chimeric transcripts, with large T-DNA inserts that contain multiple stop codons in each reading frame, which makes the synthesis of functional gene products highly unlikely.

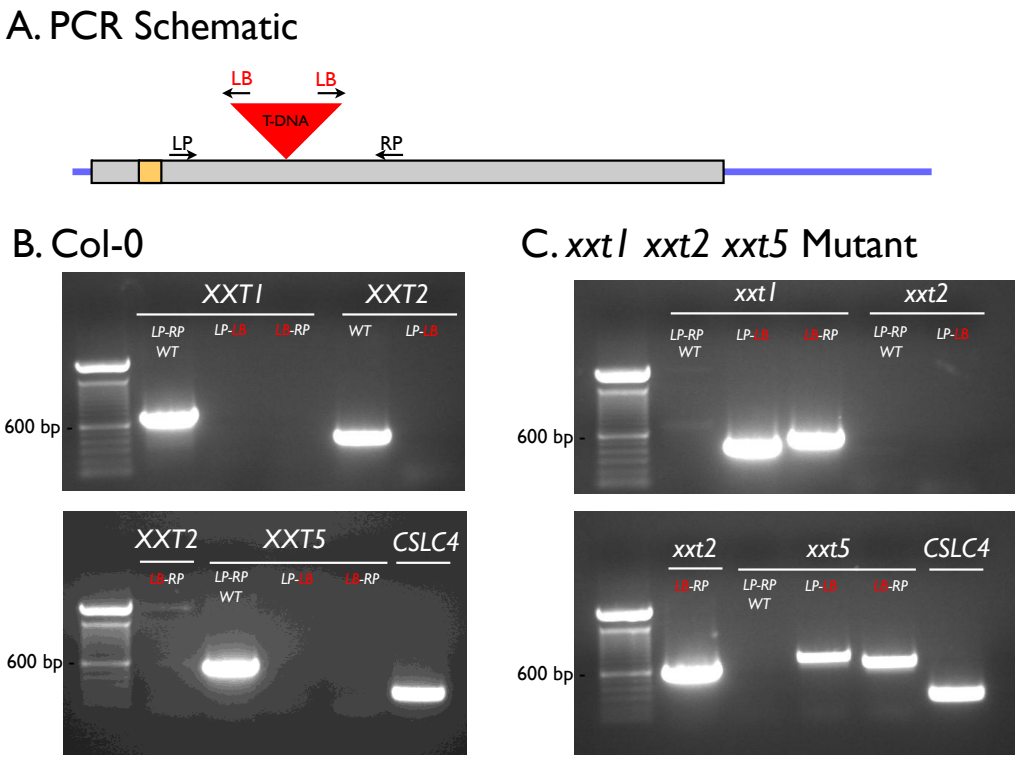

Supplemental Figure S1. RT-PCR characterization of xylosyltransferase transcripts in the Col-0 and *xxt1 xxt2 xxt5* mutant. A. Schematic of PCR strategy. Based on results from PCR and sequencing experiments of XXT T-DNA inserts (Figure 1) we characterized Col-0 and mutant transcripts using combinations of GSP left primers (LP), right primers (RP), and T-DNA-specific left boarder (LB) boarder primers. Blue line, 5' and 3' UTRs; gray bar, CDS; red triangle, T-DNA insert; orange box, putative transmembrane domain. B. PCR characterization of Col-0 *XXT1*, *XXT2*, and *XXT5* cDNA. *CSLC4*, *Cellulose Synthase-Like Family C4*, a putative xyloglucan glucan synthase (Cocuron et al., 2007). C. PCR characterization of *xxt1 xxt2 xxt5* mutant *XXT* transcripts.

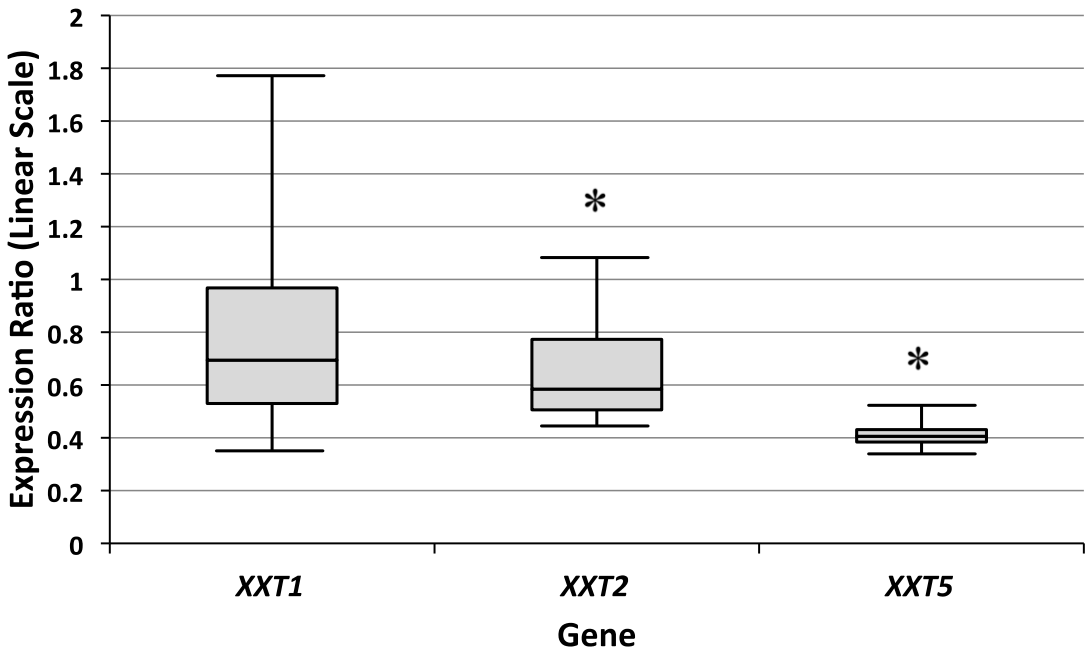

Supplemental Figure S2. Relative expression of *XXT1*, *XXT2*, and *XXT5* chimeric transcripts in the *xxt1 xxt2 xxt5* mutant versus Col-0. Transcript levels of *XXT1*, *XXT2*, *XXT5*, and *PROTODERMAL FACTOR 2* (*PDF2*; At4G04890) were measured in the *xxt1 xxt2 xxt5* mutant and Col-0 seedlings by qPCR (See Supplemental Material and Methods) of N=3 biological replications. Relative expression software tool (REST) (Pfaffl et al., 2002) was used to calculate the expression ratio of each *XXT* between the *xxt1 xxt2 xxt5* mutant and Col-0 using *PDF2* as the reference gene and 10,000 iterations to calculate statistical significance (*; $P < 0.01$).

Supplemental Materials and Methods

Total RNA was isolated from three biological reps of Col-0 and *xxt1xxt2xxt5* seedlings using (RNeasy Plant Mini Kit; Qiagen). RNA samples were digested twice with DNAse (DNA-Free kit; Ambion) and converted to cDNA with reverse transcriptase (High Capacity cDNA Reverse Transcription kit; ABI). Isolation of RNA, DNAse digestion, and RT reactions were done according to manufacturer's instructions.

For RT-PCR characterization experiments, PCR was performed on cDNA samples using combinations of gene-specific primers and T-DNA-specific primers (Supplemental Table S1) and JumpStart RED Taq ReadyMade PCR mix (Sigma-Aldrich) according to manufacture's instructions. PCR reactions, 50 µl total volume, were run at 35 cycles of 94^{o}C for 45 s, 55^{o}C for 1 min, and 72^{o}C for 2 min, and a final extension at 72^{o}C for 5 min. PCR reaction products were

separated on a 1% agarose gel containing 0.005% ethidium bromide. PCR bands were sliced out of the gel and the amplicons were purified using the Geneclean Spin Kit (Q-Biogene) according to manufacture's instructions. PCR amplicons were sequenced by the Michigan State University Research Technology Support Facility using GSP and T-DNA specific primers (Supplemental Table S1) on an ABI 3730 Genetic Analyzer.

For qPCR experiments, we followed the guidelines set forth by of (Udvardi et al., 2008), (Gutierrez et al., 2008), and (Rieu and Powers, 2009) for the analysis of transcript levels in Col-0 and the *xxt1 xxt2 xxt5* mutant. Each 50 µl qPCR reaction contained the cDNA equivalent of 100 ng of RNA, 200 nM final concentration of each primer, water, and 25 µl Power SYBR Green (ABI). qPCR reactions were analyzed on an ABI 7500 Fast Real-Time PCR System. Lack of genomic DNA contamination was confirmed with PCR using primers that flanked the 2nd intron of *CSLC4* (At3g28180) and by qPCR analysis of RT-minus reactions. Absence of primer dimers was confirmed by examination of dissociation curves. Based on recommendations and protocols detailed in Gutierrez et al. (2008) and Czechowski et al. (2005) *PROTODERMAL FACTOR 2* (*PDF2*; At4G04890) was validated as a reference gene. qPCR Δ-Rn values were imported into LinRegPCR software (Ramakers et al., 2003; Ruijter et al., 2009), which was used to calculate the baseline, PCR efficiency, and *Ct* of each PCR reaction. Relative expression software tool (REST) (Pfaffl et al., 2002) was used to determine the relative expression of each transcript with respect to *PDF2* using 10,000 randomizations to calculate statistical significance.

Supplemental Table S2: Expanded listing of all individual plant glycan-directed monoclonal antibodies (mAbs) used for glycome profiling (Figure 5). The antibody groupings are based on a hierarchical clustering analysis of all mAbs screened against a panel of plant polysaccharide preparations (Pattathil et al., 2010; 2012) that groups the mAbs according to the polysaccharides that they predominantly recognize. The majority of listings link to the Wall*MAB* DB plant cell wall monoclonal antibody database (http://www.wallmabdb.net) that provides detailed descriptions of each mAb, including immunogen, antibody isotype, epitope structure (to the extent known), supplier information, and related literature citations.

Glycan Group Recognized	mAb Names
Non-Fucosylated Xyloglucan-1	CCRC-M95 CCRC-M101
Non-Fucosylated Xyloglucan-2	CCRC-M104 CCRC-M89 CCRC-M93 CCRC-M87 CCRC-M88
Non-Fucosylated Xyloglucan-3	CCRC-M100 CCRC-M103
Non-Fucosylated Xyloglucan-4	CCRC-M58 CCRC-M86 CCRC-M55 CCRC-M52 CCRC-M99
Non-Fucosylated Xyloglucan-5	CCRC-M54 CCRC-M48 CCRC-M49 CCRC-M96 CCRC-M50 CCRC-M51 CCRC-M53
Non-Fucosylated Xyloglucan-6	CCRC-M57 CCRC-M90
Fucosylated Xyloglucan	CCRC-M102 CCRC-M39

CCRC-M106
CCRC-M84
CCRC-M1

CCRC-M111
CCRC-M108
CCRC-M109

CCRC-M119
CCRC-M115
CCRC-M110
CCRC-M105
CCRC-M117
CCRC-M113
CCRC-M120
CCRC-M118
CCRC-M116
CCRC-M114

CCRC-M75
CCRC-M70
CCRC-M74

CCRC-M38
JIM5
JIM136
JIM7
CCRC-M34

CCRC-M69
CCRC-M35
CCRC-M36
CCRC-M14
CCRC-M129
CCRC-M72

CCRC-M40
CCRC-M83
CCRC-M82

CCRC-M98
CCRC-M94


Rhamnogalacturonan-Ia
CCRC-M5
CCRC-M2
CCRC-M4
CCRC-M6
Rhamnogalacturonan-Ib
CCRC-M23
CCRC-M17
CCRC-M19
CCRC-M18
CCRC-M56
CCRC-M16
Rhamnogalacturonan-Ic
JIM137
JIM101
CCRC-M61
CCRC-M30
Rhamnogalacturonan-I
Arabinogalactan
CCRC-M60
CCRC-M41
CCRC-M80
CCRC-M79
CCRC-M44
CCRC-M33
CCRC-M32
CCRC-M13
CCRC-M42
CCRC-M24
CCRC-M12
CCRC-M7
CCRC-M77
CCRC-M25
CCRC-M9
CCRC-M128
CCRC-M126
CCRC-M125
CCRC-M123
CCRC-M122
CCRC-M121
CCRC-M112
CCRC-M21
JIM131
CCRC-M22
JIM132
JIM1

CCRC-M15
CCRC-M8
MH4.3E5
JIM16
CCRC-M10
CCRC-M11

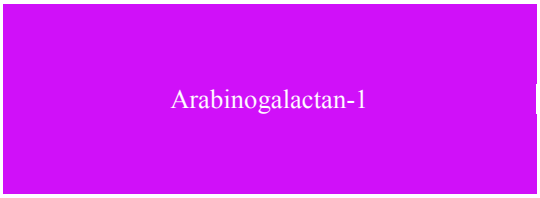

JIM93
JIM94
JIM11
MAC204
JIM20

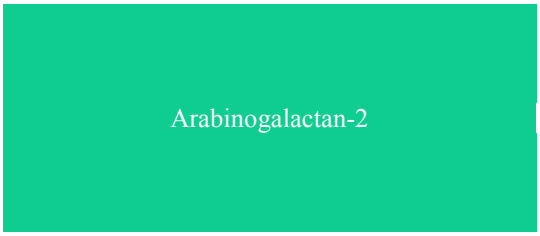

JIM14
MAC207
JIM19
JIM12
CCRC-M107

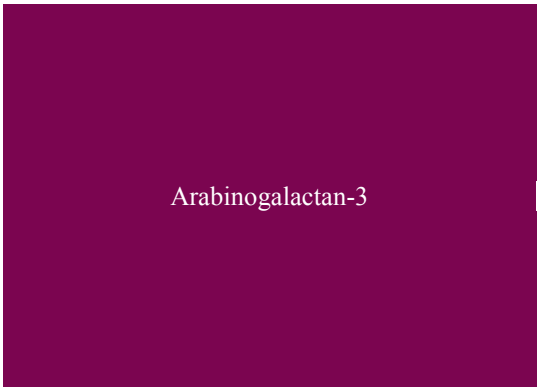

JIM4
CCRC-M31
JIM17
CCRC-M26
JIM15
JIM8
CCRC-M85
CCRC-M81
MAC266
PN16.4B4

PN16.1B3
JIM133
JIM13
CCRC-M92
CCRC-M91
CCRC-M78

MAC265
CCRC-M97

References

Cocuron JC, Lerouxel O, Drakakaki G, Alonso AP, Liepman AH, Keegstra K, Raikhel NV, Wilkerson CG. (2007). A gene from the cellulose synthase-like c family encodes a β-1, 4 glucan synthase. Proc. Natl. Acad. Sci. **104**: 8550-8555

Gutierrez L, Mauriat M, Pelloux J, Bellini C, Van Wuytswinkel O (2008). Towards a systematic validation of references in real-time rt-PCR. Plant Cell **20**: 1734-1735

Pattathil S, Avci U, Baldwin D, Swennes AG, McGill JA, Popper Z, Bootten T, Albert A, Davis RH, Chennareddy C, Dong RH, O'Shea B, Rossi R, Leoff C, Freshour G, Narra R, O'Neil M, York WS, Hahn MG. (2010) A comprehensive toolkit of plant cell wall glycan-directed monoclonal antibodies. Plant Physiology **153:** 514-525

Pattathil S, Avci U, Miller J.S, Hahn MG (2012) Immunological approaches to plant cell wall and biomass characterization: Glycome Profiling. *In* M. Himmel, ed, Biomass Conversion: Methods and Protocols. Humana Press (in press)

Pfaffl MW, Horgan GW, and Dempfle L. (2002). Relative expression software tool (REST) for group-wise comparison and statistical analysis of relative expression results in real-time PCR. Nucleic Acids Res **30**, e36

Ramakers C, Ruijter JM, Deprez RH, and Moorman AF. (2003). Assumption-free analysis of quantitative real-time polymerase chain reaction (PCR) data. Neurosci Lett **339**, 62-66.

Rieu I, and Powers SJ. (2009). Real-time quantitative RT-PCR: Design, calculations, and statistics. Plant Cell **21**, 1031-1033

Ruijter JM, Ramakers C, Hoogaars WM, Karlen Y, Bakker O, van den Hoff MJ, and Moorman AF. (2009). Amplification efficiency: Linking baseline and bias in the analysis of quantitative PCR data. Nucleic Acids Res **37**, e45

Schmid, M, Davison, T, Henz, S, Pape, U, Demar, M, Vingron, M, Schölkopf, B, Weigel, D, and Lohmann, J. (2005). A gene expression map of *Arabidopsis thaliana* development. Nat. Genet. **37**: 501-506

Udvardi MK, Czechowski T, and Scheible WR. (2008). Eleven golden rules of quantitative RT-PCR. Plant Cell **20**, 1736-1737.

Wang YH. (2008). How effective is T-DNA insertional mutagenesis in *Arabidopsis*. J. Biochem. Tech. **1**, 11-20